The formation of strong-couple interactions between nitrogen-doped graphene and sulfur/lithium (poly)sulfides in lithium-sulfur batteries

2015 2D Mater. 2 014011

(http://iopscience.iop.org/2053-1583/2/1/014011)

2D Materials

RECEIVED
19 December 2014

ACCEPTED FOR PUBLICATION
16 February 2015

PUBLISHED
16 March 2015

PAPER

The formation of strong-couple interactions between nitrogen-doped graphene and sulfur/lithium (poly)sulfides in lithium-sulfur batteries

Ting-Zheng Hou[1], **Hong-Jie Peng**[1], **Jia-Qi Huang**[1], **Qiang Zhang**[1] **and Bo Li**[2]

[1] Beijing Key Laboratory of Green Chemical Reaction Engineering and Technology, Department of Chemical Engineering, Tsinghua University, Beijing 100084, People's Republic of China

[2] Shenyang National Laboratory for Materials Science, Institute of Metal Research, Chinese Academy of Sciences, 72 Wenhua Road, 110016 Shenyang, People's Republic of China

E-mail: zhang-qiang@mails.tsinghua.edu.cn **and** boli@imr.ac.cn

Keywords: graphene, lithium-sulfur batteries, energy storage, nitrogen doped carbon

Supplementary material for this article is available online

Abstract

A lithium-sulfur battery with a very high theoretical energy density (2600 Wh kg^{-1}) is one of the most promising candidates for next-generation energy storage devices. However, there are still many problems impeding the practical use of lithium-sulfur batteries, including the 'shuttle effect' and irreversible loss of active materials. Enhancing the interfacial interaction between the carbon hosts and the sulfur-containing guests by rational nitrogen doping is an effective route. First principle calculations were performed to illustrate the adsorption behavior between sulfur/lithium (poly) sulfides and pristine/nitrogen-doped graphene nanoribbons with different edge structures. N-dopants on doped graphene nanoribbon in pyrrolic and pyridinic forms donated extra binding energies of 1.12 ~ 1.41 eV and 0.55 ~ 1.07 eV, respectively. Quaternary nitrogen enriched on the edge can benefit from the adsorption of active materials. Compared with pristine graphene nanoribbon, nitrogen-doped graphene nanoribbons exhibited strong-couple interactions for anchoring sulfur-containing species, achieving high stability and reversibility, which was consistent with experimental findings. These results shed light on the cathode design of lithium-sulfur batteries and on the potential to understand host–guest interactions in other energy storage systems.

Introduction

The energy storage system with a high energy density holds a decisive position to fulfilling the ever-increasing demands of electronic devices, electric vehicles, and smart grid for intermittent solar or wind power. A lithium-ion battery (LIB), which has a theoretical energy density of 360 Wh kg^{-1} for a routine $LiCoO_2$/graphite system, cannot fully satisfy this requirement. A lithium-sulfur (Li-S) battery, ignited by its transfer electrochemistry beyond the horizon of LIBs, is a promising candidate for next-generation energy storage [1]. It presents a theoretical energy density of 2600 Wh kg^{-1}, which is 5–7 times higher than that of conventional LIBs. Li-S batteries show advantages in high capacity 1672 mAh g^{-1} of sulfur cathode materials, abundant natural sulfur resources at low cost and low toxicity, and wide battery operating-temperature range [2–4]. The Li-S battery holds great promise for a next-generation high-energy battery owing to these distinguished advantages.

However, the practical application of Li-S batteries is impeded by a series of obstacles. Firstly, sulfur and the discharge products (Li_2S_2 of Li_2S) of Li-S batteries are intrinsically insulative. Accordingly, nanomaterial scaffold with extraordinary electrical conductivity and mechanical strength are often employed to accommodate active materials [5, 6]. Sulfur tends to adhere on these conductive frameworks (such as porous carbon [7], carbon nanotubes (CNTs) [8], carbon fibers [9], graphene [10–13], conductive polymers [14] and their hybrids [15, 16]) and accepts electrons efficiently. However, these conductive additives are unfavorable to absorb the polar lithium (poly)sulfides (Li_2S_n, $n = 1$–8). Secondly, high-order polysulfides (Li_2S_n, $n = 6$–8) can dissolve into the electrolyte, migrate to and react with the lithium anode. Then subsequently, low-order polysulfides (Li_2S_n, $n = 4$–6)

can diffuse back to the cathode. The whole circle between cathode and anode is called the 'shuttle effect', which induces self-discharge and lowers the energy efficiency. Moreover, solid lithium sulfides (Li_2S_n, $n = 1–2$) may detach from the conductive scaffolds due to the huge volume expansion/extraction during repeated circulation, resulting in irreversible deterioration of capacity. If a consummate interface can be constructed with a strong-couple interaction between the active materials and carbonscaffold host, the as-obtained Li-S battery is expected to be highly stable and reversible.

Enormous efforts have been devoted to prevent the migration of polysulfides. On one hand, ionic exchange/selective membranes [17, 18], solid electrolytes [19], 'solvent-in-salt' electrolyte [20], as well as lithium salt additives (such as $LiNO_3$) [21] were adopted to retard the dissolution, diffusion, or side reaction of lithium polysulfides. However, the extra resistance of ion migration may induce poor reaction kinetics. On the other hand, modifications of cathode structure via interlayers [22, 23], hollow sphere structures [24, 25], and polysulfide reservoirs [26] were proposed to provide physical confinement. However, these attempts mainly relied on the weak physical interactions between the carbon hosts and S-containing guests, and new strategies for the further improvement in the stability of Li-S battery should be developed. Recently, pioneering works on graphene oxides lightened a chemical-adsorption approach by using surface functional groups to immobilize sulfur and lithium polysulfides [27–30]. The strong interaction between graphene oxide and sulfur or polysulfides significantly improved the utilization of active materials and prevented the shuttle effect, which benefited Li-S cells in high reversible capacity and stable cycling [27]. Based on these considerations, if the host/guest interaction can be intensified by the chemical modification of conductive scaffolds to build a 'strong-couple interface', the 'shuttle effect' will be inhibited and therefore a stable and effective electrochemical contact will be sustained.

Introducing heteroatoms into graphene renders tunable electronic properties and therefore tunable chemical reactivities. Nitrogen is a very critical element that bears five valence electrons, which is different from carbon. Such heteroatoms in a graphene lattice can even act as a Lewis base and interact with other molecules. N-doped CNTs [9, 31–34] and N-doped porous carbon [35, 36] were employed as conductive hosts, which play an important role for the dynamic interface between the chemically modified carbon hosts and S-containing guests for stable Li-S batteries. Subsequently, N-doped graphene, with promoted chemical adsorption capability for sulfur, attracted even more attention, leading to a high reversibility and stability for Li-S battery use [12, 37, 38]. All the above studies demonstrated that N-doped nanocarbon materials could promote the practical performance of the carbon network experimentally. But the interfacial chemical properties, especially the detailed role of N-dopants, are still worthy of being explored and systematically investigated.

In this contribution, we present a theoretical investigation of the interaction between N-doped graphene nanoribbons (GNRs) and all of the S-containing species involved in the charge and discharge process of a practical Li-S cell. First principle calculations were adopted for their ability to atomically understand the interfacial interaction in a microscopic view. Two-dimensional (2D) graphene were selected as the model system for its wide application in energy storage. The non-polar sulfur molecule and the polar lithium (poly)sulfides were allowed to interact with these 2D materials, showing the atomic interactions at the interfaces. The binding state of N-dopants, geometrical configuration and edge structure of GNRs were systematically investigated, showing their effects on adsorption energy and how N-doped graphene provide a strong-couple interface with S-containing guest molecules.

Computational methods

Theoretically, there are hexagonal network structures infinitely extended in two dimensions in an ideal piece of graphene. However, there are usually abundant edges and boundaries where heteroatoms (e.g. hydrogen, nitrogen, oxygen, boron) are enriched. In light of chemical doping, the edge of a graphene plane is modified. Thus, the 2D graphene material is endowed with unique properties to preferably interact with sulfur-containing clusters involved in the electrochemical process. Herein, a first principles calculation is conducted to systematically investigate the interaction between the un-/N-doped nanocarbon materials and the S-containing species (Li_2S, Li_2S_4, Li_2S_8 and S_8, in particular).

GNR was selected as a model system because of its simple plane structure of 2D graphene honeycomb lattice and two typical edge configurations of zigzag edge and armchair edge. There are also N-dopants with different configurations in a doped GNR. Based on the high resolution N1s spectrum of x-ray photoelectron spectroscopy results, quaternary-N, pyridinic-N, and pyrrolic-N were the dominant forms of N-dopants. In our case, the edge structure together with the N-dopants was tuned for seven kinds of GNRs, namely, pristine zigzag nanoribbon (Z1), zigzag nanoribbon with quaternary nitrogen (Z2), zigzag nanoribbon with pyridinic nitrogen (Z3), pristine armchair nanoribbon (A1), armchair nanoribbon with quaternary nitrogen (A2), armchair nanoribbon with pyridinic nitrogen (A3), and armchair nanoribbon with pyrrolic nitrogen (A4). The edges of GNRs were saturated with hydrogen atoms to compensate the valence of carbon atoms. Li_2S, Li_2S_4, Li_2S_8 clusters and S_8 molecules were

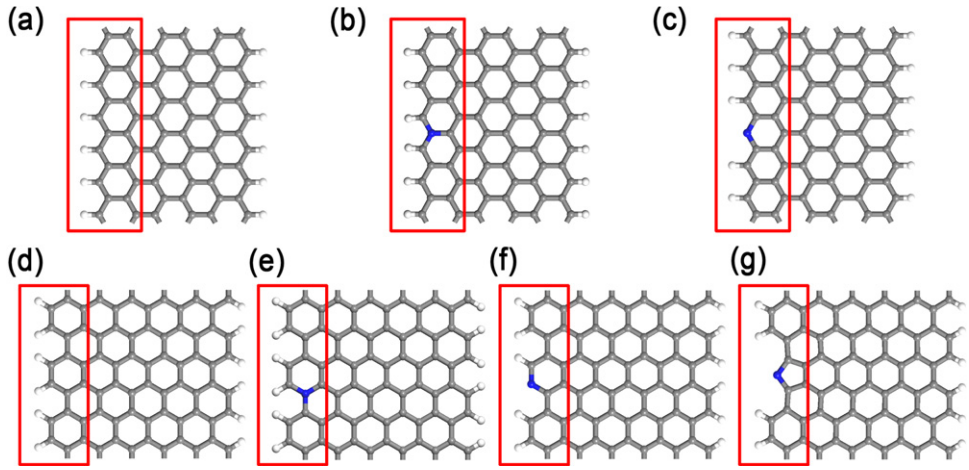

Figure 1. The PBE-level optimized configuration of (a) pristine zigzag GNR (Z1), (b) zigzag GNR with quaternary nitrogen (Z2), (c) zigzag GNR with pyridinic nitrogen (Z3), (d) pristine armchair GNR, (e) armchair GNR with quaternary nitrogen (A2), (f) armchair GNR with pyridinic nitrogen (Z3), (g) armchair GNR with pyrrolic nitrogen (Z4). The carbon, hydrogen and nitrogen atoms are denoted as spheres in grey, white, and blue, respectively, while the red rectangles represent the region where Li_2S, Li_2S_4, Li_2S_8 and S_8 are supposed to interact with the nanoribbons.

allowed to interact with the edges of these seven kinds of GNRs.

The calculation is based on density functional theory (DFT), using the Perdew–Burke–Ernzerhof (PBE) exchange-correlation functional [39] in the framework of the general gradient approximation (GGA) implemented in the DMol3 package in Materials Studio [40, 41] (version 5.5) of Accelrys Inc. An all-electron double numerical basis set with polarization functions (DNP basis set) was used in this contribution. The convergence criteria applied for geometry optimizations were 2.0×10^{-5} au, 4.0×10^{-3} au Å^{-1}, and 5.0×10^{-3} Å for energy change, maximum force, and maximum displacement, respectively. The threshold for self-consistent-field (SCF) density convergence was set to 1.0×10^{-5} eV. The K point was set to $8\times1\times1$, which was verified by the convergence test as shown in figure S1 (available in the supplementary data). The vacuum layer along the normal direction and the slip direction of the nanoribbon was set to 20 Å, which was examined to be large enough to avoid an unexpected interaction between atoms in different super cells. Each pristine nanoribbon was added with one nitrogen atom per 72 carbon atoms, corresponding to a nitrogen atomic concentration of 1.4%. As described above, substitutional impurities tend to concentrate on the edge. To further testify the predominant substitutional site of N-dopants, two structural models of nanoribbon with quaternary-N on two different substitutional sites were tested, which are shown in figure S2 (available in the supplementary data). The result indicated that the quaternary-N energetically preferred to lie on the edge.

The optimized configurations of each modeled nanoribbon are shown in figure 1. The red rectangles presented the region where Li_2S, Li_2S_4, Li_2S_8 and S_8 were supposed to interact with the dopant with different forms located at the edges of nanoribbons. For a quantitatively description of the interactions between the nanoribbons and the S-containing clusters, the binding energy E_b was defined as follows:

$$E_b = E(\text{total}) - (E(C) + E(S)). \quad (1)$$

E(C), E(S) and E(total) represent the total energies of a nanoribbon, an isolated sulfur-containing cluster (Li_2S, Li_2S_4, Li_2S_8 clusters or S_8 molecule), and a certain nanoribbon binding to a S-containing cluster, respectively. The higher absolute value of binding energy corresponds to stronger interaction.

Results and discussion

The binding energies of S-containing clusters interacting with nanoribbons are summarized in figure 2 and table S1, S2 (available in the supplementary data). For pristine GNRs with zigzag and armchair edges, lithium (poly)sulfides exhibited higher binding energies as the length of (poly)sulfide chains decreased. However, all of the binding energies of polar S-containing clusters adsorbed on pristine GNRs were 0.76–1.12 eV, which are lower than that of the non-polar S_8 molecule. Therefore, we can assume that once the S_8 molecule accepted lithium ions and reduced to soluble lithium (poly)sulfides, the sulfur element cannot recover to the favorable initial binding state to GNRs in the form of the S_8 molecules. This is direct proof that the high-order polysulfides would suffer from remarkable nonreciprocal loss due to the dissolution and related shuttle effect. Even when low-order polysulfides shuttled back to the cathode, they may not be fully reused due to the poor affinity to conducting carbon surface.

The dissolution of polysulfides is widely detected in a routine Li-S cell with C/S cathode. The

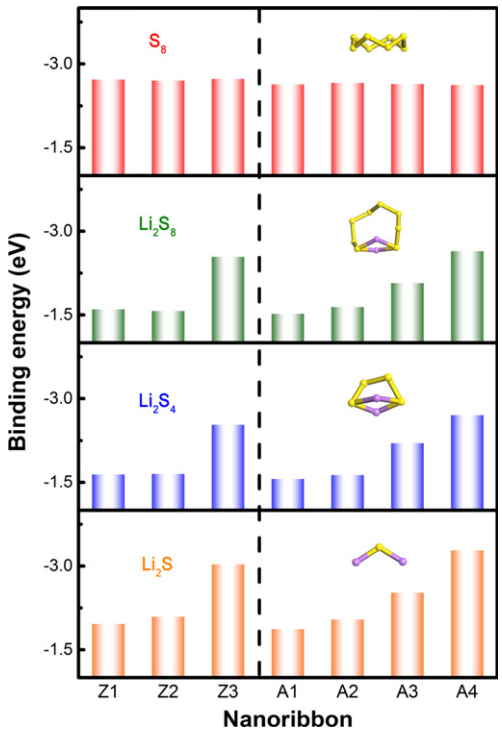

Figure 2. The binding energy (eV) of S_8, Li_2S_8, Li_2S_4 and Li_2S (length of (poly)sulfide chains in descending order) interacting with Z1-Z3 GNRs with zigzag edges and A1–A4 GNRs with armchair edges. The optimized configuration of S_8, Li_2S_8, Li_2S_4 and Li_2S are also provided as inset figures. The lithium and sulfur atoms are denoted as spheres in purple and yellow, respectively.

modification of the graphene through N-doping is effective to retard the dissolution of polysulfides and related polysulfide shuttle [42, 43]. During the charge and discharge process, the N-doped carbon materials can trap the soluble polysulfide intermediates. According to our theoretical prediction results, all the edges of GNRs exhibited similar binding energy ($-2.65 \sim -2.76$ eV) for the case of S_8, illustrating that the binding state of non-polar S_8 molecules were obtuse to the configuration of the edge and almost immune to the introduction of N-dopants. However, the polar species were quite sensitive to different edges based on the corresponding binding energy of the lithium (poly)sulfides. Both Z3 and A3 with pyridinic-N showed relatively larger binding energies ($-2.57 \sim -3.06$ eV, $-2.10 \sim -2.55$ eV) with lithium polysulfides, which was contrasted with the much lower binding energies ($-1.63 \sim -1.99$ eV, $-1.55 \sim -1.90$ eV) of Z1 and A1 GNRs with pristine edges. The pyridinic-N exhibited strong affinity with lithium polysulfides, raising the binding energy by $0.55 \sim 1.07$ eV. The experimental results collected by the UV/vis spectroscopy have confirmed these phenomena [42]. The concentration of Li_2S_6 in an ether-type electrolyte solution added with N-doped graphene was lower than that with pristine graphene, suggesting a larger adsorption amount of polysulfides by providing additional adsorption sites. Furthermore, the x-ray absorption spectroscopy measurement on N-doped graphene/S cathode after 200 charge/discharge cycles showed a new peak in the N K-edge spectrum, supporting the positive involvement of N-functional groups for lithium sulfide immobilization [43].

The different binding states were validated by not only the value of binding energy but also the donation and acceptance of the electron around the local binding sites with specific geometry of S-containing clusters. In particular, the optimized configuration and deformation charge density corresponding to the Li_2S adsorption site on the seven nanoribbons are shown in figure 3, in which the increase and decrease of total electron density with the density of isolated atoms subtracted are denoted as blue and red, respectively. The state of individual Li_2S is provided in figure 3(a) for reference. For pristine GNRs (Z1 and A1), there were no obvious concentration of electron density between Li_2S and un-doped carbon scaffolds according to figures 3(b) and (e). Meanwhile, the Li-S-Li chain was approximately perpendicular to the 2D graphene plane with no obvious redistribution of electrons which were still concentrated around the central S atoms as the initial isolated state. All of the above phenomena indicate an extremely weak electrostatic interaction between Li_2S and un-doped GNR edges. It can be suspected accordingly that Li_2S may difficultly re-deposit from polysulfides or easily detach from the conductive scaffolds in a real Li-S cell. However, such interaction was significantly intensified by introducing pyridinic-/pyrolic-N into graphene lattice. Figure 3(d) is a typical demonstration describing the optimized configuration of Li_2S binding with zigzag edge with pyridinic-N (Z3). In the most stable configuration, terminal Li atoms in Li_2S tended to directly bind to the pyridinic-N atom in Z3. There was distinctive electron concentration between N and Li atoms, suggesting a strong Li–N electrostatic interaction. The electron migration can be well explained by the Lewis acid-base theory. The pyridinic-N with an extra pair of electrons was considered as an electron-rich donor that naturally acted as a Lewis-base site to interact with the strong Lewis acid of terminal Li atom in lithium (poly) sulfides. Moreover, by carefully comparing the deformation charge density of Li-S-Li in figure 3(a) and Li-S-Li $\cdots$ N in figure 3(d), the electron slightly moved from the S-Li bond to the bridged Li-N pair, due to the higher electronegativity of the N atom (3.066) than the S atom (2.589). Thus, as a strong Li-N interaction was formed, the S-Li bond was relatively weakened. Therefore, a strong-couple interaction exists, which is hardly influenced by the edge structure (figure 3(g)). As similarly indicated in figure 3(h), pyrrolic-N played an analogous role as pyridinic-N.

Compared to the C atom in a graphene lattice, quaternary-N is an electron-rich donor and could increase the local charge density at doping region.

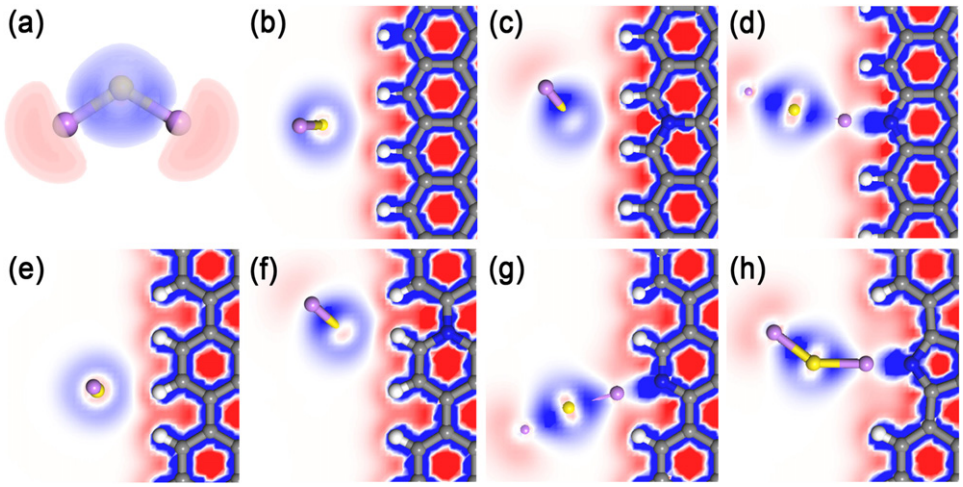

Figure 3. The optimized configuration and corresponding deformation charge density of (a) Li_2S and the Li_2S adsorption site of (b) Z1, (c) Z2, (d) Z3, (e) A1, (f) A2, (g) A3, and (h) A4. The increase/decrease of total electron density with the density of isolated atoms subtracted is denoted as blue/red, respectively.

However, different from pyridinic-/pyrrolic-N, quaternary-N with saturated electron orbitals is not able to afford an extra lone pair electron for adsorbing Li_2S. Hence the mechanism on the improvement by quaternary-N doped GNRs (Z2 and A2) might differ from the direct-binding mechanism of Li-N interaction in Z3 and A3–A4. Quantitatively, the quaternary-N enabled the S-containing polar species to link more easily with the edge of the conductive skeleton. The binding energies of Z2 and A2 ($-1.60 \sim -2.12$ eV and $-1.67 \sim -2.07$ eV, respectively) were slightly larger than the pristine ones. The reason can mainly be ascribed to different polarity at the edges of pristine GNRs (Z1 and A1 in figures 3(b) and (e)) and quaternary-N-doped GNRs (Z2 and A2 in figures 3(c) and (f)). On one hand, the quaternary-N in graphene plane served as an electron donor that provided two electrons to the π-conjugated system. On the other hand, as the electronegativity of the N atom (3.066) is higher than that of the C atom (2.55) and H atom (2.20), quaternary-N can attract an electron from adjacent atoms. Consequently, the electron distribution modified by quaternary-N fulfilled the edge with higher polarity and dipole moment, which was validated by electron population analysis. As a result, the polar Li_2S clusters suffered from a stronger Keesom force. This effect might be magnified by improving the density of quaternary-N dopants in a local region. Nevertheless, in terms of the value of binding energy, the role of quaternary-N was not that active as pyridinic-/pyrrolic-N. This can be rationalized by regarding the graphene plane as a conjugated system. The electron originated from the nitrogen was highly delocalized on the whole plane according to figures 3(c) and (f). Hence, the potential ability for the *p* electron pair to attractive lithium (poly)sulfides was concealed on the right site where a carbon was substituted by a quaternary-N.

The interaction behaviors of zigzag and armchair edges were quite similar to each other. Notably, all else being equal, the binding energy of the armchair edge was slightly ($0.02 \sim 0.09$ eV) smaller than that of the zigzag edge. Interpreted by figure 3, the difference was induced by different arrangements of hydrogen at the edges. In figures 3(b), (c), each hydrogen atom was periodically distributed on the zigzag edge. There was close contact with two hydrogen atoms for the sulfur atom in Li_2S. However, as shown in figures 3(e), (f), the hydrogen atoms distributed non-equidistantly and had an angle between each other on the armchair edge, which hindered the interaction between the Li_2S guest and the carbon host.

Due to geometric constraints, a pentagon ring was not considered at the zigzag edge to accommodate pyrrolic-N. Consequently, pyrrolic-N was only built on the armchair edge. Compared with pyridinic-N, pyrrolic-N exhibited even higher binding energies ($-2.67 \sim -3.31$ eV) to immobilize lithium (poly)sulfides, which were $1.12 \sim 1.41$ eV higher than those of the pristine nanoribbons. This can be explained by the deformation charge density shown in figures 3(d), (g) and (h). Li atoms in Li_2S formed even more concentrated charge density with pyrrolic-N than pyridinic-N, in accordance with the stronger interaction. Except for local deformation charge density, the steric effect is another important factor that influences the interaction behavior. As shown in figure 4, the distances between the two hydrogen neighboring the pyrrolic-N on armchair edge, pyridinic-N on zigzag edge, and pyridinic-N on armchair edge were 5.84, 4.75, and 4.03 Å, respectively, which was in good accordance with the binding energy in a descending trend (-3.31 eV to -2.55 eV). Thus, a more open space formed by pyrrolic-N was expected to favor the strong-couple interaction with S-containing guests.

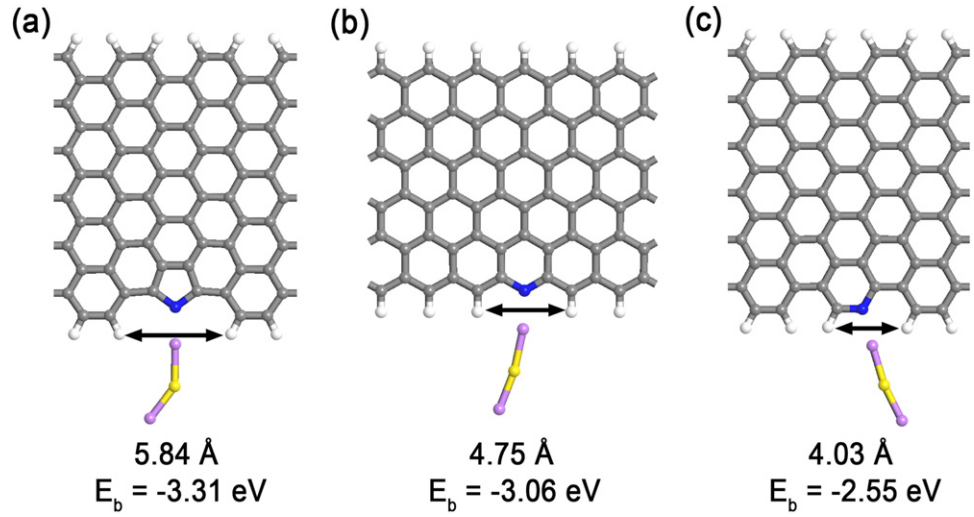

Figure 4. The optimized configuration and the corresponding binding energy based on the first principles calculation of Li_2S adsorbed by (a) A4, (b) Z3 and (c) A3. Lines with arrowheads show the length between the two hydrogen atoms nearest to pyrrolic-/pyridinic-N.

N-doping essentially tuned the surface properties of graphene hosts, especially the properties embodied by the edge, to afford a highly active interface. Benefiting from appropriate N-doping, a chemical gradient for effectively trapping the soluble lithium polysulfides was built by pyrrolic-/pyridinic-N. Meanwhile, Li_2S, the end product of discharge, was also well confined on the surface, avoiding the incapability of detached Li_2S to be recharged. This was desirable for effectively preventing shuttle effect and achieving high capacity and high coulombic efficiency. Our theoretical results coincided well with another theoretical prediction that N-dopant in nanocarbon can provide active sites for immobilizing lithium (poly)sulfides [37, 42, 43]. While experimentally, N-doped graphene paper electrode exhibited a high specific capacity of approximately 1000 mAh g^{-1} after 100 cycles and excellent coulombic efficiency of 98% for the catholyte-type Li-S cell [42]. N-doped graphene also enabled the sulfur composite cathode to deliver high specific discharge capacities of 1167, 1058, 971, 802, 606 mAh g^{-1} at a current rate of 0.2, 0.5, 1.0, 2.0, 5.0 C, respectively. The Li-S cell also realized a much extended cycle life over 2000 cycles and an extremely low capacity-decay rate of 0.028% per cycle [43]. Benefiting from N-doping and correspondingly enhanced interfacial interaction, the practical performance of N-doped graphene as cathode host for Li-S batteries was significantly better than that of un-doped graphene. The theoretical prediction and the experimental result corroborated well with each other to a very large extent, fully vindicating that chemical modification can significantly increase the interaction between the host and the guest. Such strong-couple interaction guarantees a stable and effective interface for electrochemical reaction and phase conversion, which is vitally important for the high capacity, high stability and high reversibility of Li-S batteries.

Conclusions

Chemically doped by nitrogen, the surface chemistry of GNR, especially the adsorption property for S-containing molecules, were remarkably intensified to form a strong-couple host-guest interaction for a Li-S battery. Pyridinic-N in GNRs can afford an extra binding energy of $0.55 \sim 1.07$ eV to polar lithium (poly)sulfides due to strong electrostatic interaction between terminal Li atoms and its residual electron pair. Pyrrolic-N shows analogous intensified interaction with polar lithium (poly)sulfides but even more effective, which raised the binding energy by $1.12 \sim 1.41$ eV. Quaternary-N that preferred to locate at the edge can also make a difference for retaining the active materials, by improving the intermolecular force through enhanced polarity on the edge of the GNR plane. The binding energies corresponding to the zigzag and armchair edge were slightly different because of their different hydrogen-terminated edge. Consequently, soluble lithium polysulfide intermediates or solid Li_2S could be effectively trapped around N-doping sites. This was theoretically anticipated and experimentally demonstrated for effective inhibiting of the shuttle effect and remaining high capacity and high coulombic efficiency of the Li-S battery. The extensive inspection of N-doped GNR reported herein, especially the specific role of various N-dopants, fully addressed the importance of doping promoted chemical adsorption. These results also enlightened the understanding of interfacial phenomenon in a Li-S battery, which may also guide the rational design of cathode skeleton with strong-couple

interactions for better Li-S batteries. Such a generalized model can even be applied for the development of other energy storage systems.

Acknowledgments

This work was supported by the National Natural Science Foundation of China (21306103 and 21422604).

Reference

[1] Manthiram A, Fu Y, Chung S-H, Zu C and Su Y-S 2014 *Chem. Rev.* **114** 11751–87
[2] Yin Y-X, Xin S, Guo Y-G and Wan L-J 2013 *Angew. Chem. Int. Ed.* **52** 13186–200
[3] Chen L and Shaw L L 2014 *J. Power Sources* **267** 770–83
[4] Xu G Y, Ding B, Pan J, Nie P, Shen L F and Zhang X G 2014 *J. Mater. Chem.* A **2** 12662–76
[5] Yang Y, Zheng G and Cui Y 2013 *Chem. Soc. Rev.* **42** 3018–32
[6] Wang D W, Zeng Q C, Zhou G M, Yin L C, Li F, Cheng H M, Gentle I and Lu G Q 2013 *J. Mater. Chem.* A **1** 9382–94
[7] Ji X, Lee K T and Nazar L F 2009 *Nat. Mater.* **8** 500–6
[8] Cheng X B, Huang J Q, Zhang Q, Peng H J, Zhao M Q and Wei F 2014 *Nano Energy* **4** 65–72
[9] Li Q, Zhang Z A, Guo Z P, Lai Y Q, Zhang K and Li J 2014 *Carbon* **78** 1–9
[10] Lu S T, Cheng Y W, Wu X H and Liu J 2013 *Nano Lett.* **13** 2485–9
[11] Zhou G, Yin L-C, Wang D-W, Li L, Pei S, Gentle I R, Li F and Cheng H-M 2013 *ACS Nano* **7** 5367–75
[12] Wang X W, Zhang Z, Qu Y H, Lai Y Q and Li J 2014 *J. Power Sources* **256** 361–8
[13] Zhao M Q, Zhang Q, Huang J Q, Tian G L, Nie J Q, Peng H J and Wei F 2014 *Nat. Commun.* **5** 3410
[14] Wang J, He Y-S and Yang J 2015 *Adv. Mater.* **27** 569–75
[15] Zhao M Q, Liu X F, Zhang Q, Tian G L, Huang J Q, Zhu W C and Wei F 2012 *ACS Nano* **6** 10759–69
[16] Peng H J, Huang J Q, Zhao M Q, Zhang Q, Cheng X B, Liu X Y, Qian W Z and Wei F 2014 *Adv. Funct. Mater.* **24** 2772–81
[17] Huang J-Q, Zhang Q, Peng H-J, Liu X-Y, Qian W-Z and Wei F 2014 *Energy Environ. Sci.* **7** 347–53
[18] Bauer I, Thieme S, Bruckner J, Althues H and Kaskel S 2014 *J. Power Sources* **251** 417–22
[19] Lin Z and Liang C 2015 *J. Mater. Chem.* A **3** 936–58
[20] Suo L M, Hu Y S, Li H, Armand M and Chen L Q 2013 *Nat. Commun.* **4** 1481
[21] Aurbach D, Pollak E, Elazari R, Salitra G, Kelley C S and Affinito J 2009 *J. Electrochem. Soc.* **156** A694–702
[22] Su Y-S and Manthiram A 2012 *Nat. Commun.* **3** 1166
[23] Zhou G M, Pei S F, Li L, Wang D W, Wang S G, Huang K, Yin L C, Li F and Cheng H M 2014 *Adv. Mater.* **26** 625–31
[24] Jayaprakash N, Shen J, Moganty S S, Corona A and Archer L A 2011 *Angew. Chem. Int. Ed.* **50** 5904–8
[25] Peng H-J, Liang J, Zhu L, Huang J-Q, Cheng X-B, Guo X, Ding W, Zhu W and Zhang Q 2014 *ACS Nano* **8** 11280–9
[26] Ji X, Evers S, Black R and Nazar L F 2011 *Nat. Commun.* **2** 325
[27] Ji L W, Rao M M, Zheng H M, Zhang L, Li Y C, Duan W H, Guo J H, Cairns E J and Zhang Y G 2011 *J. Am. Chem. Soc.* **133** 18522–5
[28] Zhang C, Lv W, Zhang W, Zheng X, Wu M-B, Wei W, Tao Y, Li Z and Yang Q-H 2014 *Adv. Energy Mater.* **4** 1301565
[29] Zhou W D, Chen H, Yu Y C, Wang D L, Cui Z M, DiSalvo F J and Abruna H D 2013 *ACS Nano* **7** 8801–8
[30] Rong J P, Ge M Y, Fang X and Zhou C W 2014 *Nano Lett.* **14** 473–9
[31] Tang C, Zhang Q, Zhao M Q, Huang J Q, Cheng X B, Tian G L, Peng H J and Wei F 2014 *Adv. Mater.* **26** 6100–5
[32] Wang Z G, Niu X Y, Xiao J, Wang C M, Liu J and Gao F 2013 *RSC Adv.* **3** 16775–80
[33] Li Y C, Mi R, Li S M, Liu X C, Ren W, Liu H, Mei J and Lau W M 2014 *Int. J. Hydrogen Energy* **39** 16073–80
[34] Peng H J, Hou T Z, Zhang Q, Huang J Q, Cheng X B, Guo M Q, Yuan Z, He L Y and Wei F 2014 *Adv. Mater. Interfaces* **1** 1400227
[35] Sun F G, Wang J T, Chen H C, Li W C, Qiao W M, Long D H and Ling L C 2013 *ACS Appl. Mater. Interfaces* **5** 5630–8
[36] Song J X, Xu T, Gordin M L, Zhu P Y, Lv D P, Jiang Y B, Chen Y S, Duan Y H and Wang D H 2014 *Adv. Funct. Mater.* **24** 1243–50
[37] Wang Z Y, Dong Y F, Li H J, Zhao Z B, Wu H B, Hao C, Liu S H, Qiu J S and Lou X W 2014 *Nat. Commun.* **5** 5002
[38] Wang C, Su K, Wan W, Guo H, Zhou H H, Chen J T, Zhang X X and Huang Y H 2014 *J. Mater. Chem.* A **2** 5018–23
[39] Perdew J P, Burke K and Ernzerhof M 1996 *Phys. Rev. Lett.* **77** 3865–8
[40] Delley B 1990 *J. Chem. Phys.* **92** 508–17
[41] Delley B 2000 *J. Chem. Phys.* **113** 7756–64
[42] Han K, Shen J, Hao S, Ye H, Wolverton C, Kung M C and Kung H H 2014 *Chem. Sus. Chem.* **7** 2545–53
[43] Li W *et al* 2014 *Nano Lett.* **14** 4821–7